Towards Joint Intent Detection and Slot Filling via Higher-order Attention

Dongsheng Chen[1], **Zhiqi Huang**[1], **Xian Wu**[2], **Shen Ge**[2], **Yuexian Zou**[1, 3*]
[1]ADSPLAB, School of ECE, Peking University, China
[2]Tencent, China
[3]Peng Cheng Laboratory, China
chends@stu.pku.edu.cn, {zhiqihuang, zouyx}@pku.edu.cn, {kevinxwu, shenge}@tencent.com

Abstract

Intent detection (ID) and Slot filling (SF) are two major tasks in spoken language understanding (SLU). Recently, attention mechanism has been shown to be effective in jointly optimizing these two tasks in an interactive manner. However, latest attention-based works concentrated only on the first-order attention design, while ignoring the exploration of higher-order attention mechanisms. In this paper, we propose a BiLinear attention block, which leverages bilinear pooling to simultaneously exploit both the contextual and channel-wise bilinear attention distributions to capture the second-order interactions between the input intent or slot features. Higher and even infinity order interactions are built by stacking numerous blocks and assigning Exponential Linear Unit (ELU) to blocks. Before the decoding stage, we introduce the Dynamic Feature Fusion Layer to implicitly fuse intent and slot information in a more effective way. Technically, instead of simply concatenating intent and slot features, we first compute two correlation matrices to weight on two features. Furthermore, we present Higher-order Attention Network (HAN) for the SLU tasks. Experiments on two benchmark datasets show that our approach yields improvements compared with the state-of-the-art approach. We also provide discussion to demonstrate the effectiveness of the proposed approach.

Introduction

Spoken language understanding (SLU) that aims to understand user commands typically consists of Intent detection (ID) and Slot filling (SF) tasks. As shown in Table 1, given an utterance *"I want to listen to Hey Jude by The Beatles"*, ID can be seen as a classification task which recognizes that the user's intent is *"Play Song"*, and SF can be treated as a sequence labeling task to produce a slot label sequence in BIO format (Ramshaw and Marcus 1995; Zhang and Wang 2016) which demonstrate that *"Hey Jude"* and *"The Beatles"* are, respectively, the song's title and the artist's name that the user would like to listen.

Though ID and SF tasks can be considered separately (Liu and Lane 2016; Zhang et al. 2016, 2017; Xia et al. 2018), they have a strong correlation, e.g., once we know that the user's intent is *"Play Song"*, it would be easier for us to predict the slot labels of *"Hey Jude"* and *"The Beatles"*, and vice versa. Based on this, some works proposed to jointly model them for better performance (Goo et al. 2018; Niu et al. 2019; Qin et al. 2019; Huang, Liu, and Zou 2020; Zhou et al. 2020; Qin et al. 2021). One of the effective methods of jointly modeling SLU is the attention-based method (Li, Li, and Qi 2018; Qin et al. 2019, 2021), which adopts the attention mechanism (Vaswani et al. 2017) to trigger the mutual interaction between intent features and slot features. Specifically, the attention mechanism learns a set of weights to reflect the importance of different words of an utterance via linearly fusing the given query and key by element-wise sum, the weights are then applied to the values to derive a weighted sum which represents the enhanced intent or slot features in a mutual way.

Qin et al. (2021) proposed the *Co-Interactive* model to trigger the interaction between intent and slot features via attention, and it achieved the state-of-the-art result recently. However, we argue that the design of conventional attention inherently exploits only the first-order feature interactions and is thus inefficient. To build higher-order feature interactions, we start our exploration from second-order feature interactions via bilinear pooling, which is an operation to calculate outer product between two feature vectors. Such technique enables the second-order feature interactions by taking all pair-wise interactions between query and key into account and thus provide more discriminative representations, which has been successfully applied in the field of Computer Vision research (Lin, RoyChowdhury, and Maji 2015; Fukui et al. 2016; Chen, Deng, and Hu 2019).

Next, we introduce the BiLinear attention block illustrated in Figure 2 to build the second-order interactions between intent and slot features, and it is used to replace the conventional attention. A stack of such blocks is readily grouped to go beyond bilinear models and extract higher-order interactions is also appealing. By equipping the block with Exponential Linear Unit (ELU) (Barron 2017), the model can build infinity-order feature interactions. Besides, we proposed a more effective way to fuse intent and slot features by computing two weight matrices and weighting the features, instead of simply concatenating the intent and slot features as in the conventional approach, which is called the Dynamic Feature Fusion. Finally, we present the Higher-order Attention Network (HAN) to leverage higher-order interactions for the SLU task, namely the proposed approach, which is shown in Figure 1(b).

*Corresponding Author.

Utterence	I	want	to	listen	to	Hey	Jude	by	The	Beatles
Slot	O	O	O	O	O	B-song	I-song	O	B-artist	I-artist
Intent	Play Song									

Table 1: Example of SLU output for an utterance, which indicates the slot label sequence of an utterance with an intent *Play Song*. Slot labels are in BIO format: B indicates the start of a slot span, I indicates the inside of a span while O denotes that the word does not belong to any slot.

Extensive experiments on three baselines and two datasets proves the effectiveness of our approach. And BERT (Devlin et al. 2019), a powerful pre-trained language model, is employed to further boost the performance of our framework. We also give wide analysis to show that the introduced BiLinear attention block helps improving SLU model in robustness and generalization capability.

Overall, the main contributions of our work are as follows:

- We introduce BiLinear attention block and HAN for building higher-order attention-based SLU model. The HAN achieves new state-of-the-art results on two benchmark datasets SNIPS (Coucke et al. 2018) and ATIS (Hemphill, Godfrey, and Doddington 1990).
- We give an elegant framework of how the BiLinear attention block could be extended for mining higher or even infinity-order interactions and how to integrate such block(s) into SLU models.
- Thorough experimental results prove the effectiveness of the higher-order attention for the SLU models in terms of robustness and generalization ability.

Approach

In this section, we first describe conventional approach for SLU task, and then give the proposed approach in detail. Conventional approach consists of four parts, i.e., Self-attentive Embedder, Co-Interactive Attention Layer (CAL), Feature Fusion Layer (FFL) and SLU Decoder. The Self-attentive Embedder will process the sequence of word embeddings to get the intent and slot features. Next, the intent and slot features are both fed into the following CAL and FFL to trigger the feature interactions to enhance both of them. Finally, we use the conventional SLU Decoder to predict the intent label and slot label sequence. To build higher-order features interaction, we propose Higher-order Attention Layer (HAL) to replace the CAL, the HAL can build higher-order feature interactions. In order to enhance the features further, we propose the Dynamic Feature Fusion Layer (DFFL) to replace the FFL. The comparison of the two approach is shown in Figure 1.

Conventional Approach

Conventional approach is shown in Figure 1(a), which consists of four parts, i.e., Self-attentive Embedder, Co-Interactive Attention Layer (CAL), Feature Fusion Layer (FFL) and SLU Decoder, we will give a brief description of them.

Self-attentive Embedder Inspired by Qin et al. (2019), we employ the Self-attentive Embedder to obtain the utterance embeddings. It first uses a shared BiLSTM to embed the input utterance, acquiring $\mathbf{H} = (\mathbf{h}_1, \mathbf{h}_2, ..., \mathbf{h}_n)$. Then, it performs label attention (Cui and Zhang 2019) over intent and slot labels to get the explicit intent and slot representation:

$$\begin{aligned} \mathbf{H_I} &= \mathbf{H} + \mathrm{softmax}(\mathbf{H}\mathbf{W^I})\mathbf{W^I}, \\ \mathbf{H_S} &= \mathbf{H} + \mathrm{softmax}(\mathbf{H}\mathbf{W^S})\mathbf{W^S}, \end{aligned} \tag{1}$$

where $\mathbf{W^I} \in \mathbb{R}^{d \times |\mathbf{I}^{label}|}$ and $\mathbf{W^S} \in \mathbb{R}^{d \times |\mathbf{S}^{label}|}$ (d represents the hidden dimension; $|\mathbf{I}^{label}|$ and $|\mathbf{S}^{label}|$ represents the number of intent and slot labels, respectively). Thus $\mathbf{H_I} \in \mathbb{R}^{n \times d}$ and $\mathbf{H_S} \in \mathbb{R}^{n \times d}$ capture the intent and slot semantic information, respectively.

Co-Interactive Attention Layer (CAL) Given the query $\mathbf{q}$, we can obtain the attention distribution α over a set of keys $\mathbf{K} = \{\mathbf{k}_i\}_{i=1}^n$:

$$a_i = \mathbf{W}_a[\tanh(\mathbf{W}_k\mathbf{k}_i + \mathbf{W}_q\mathbf{q})], \alpha = \mathrm{softmax}(\mathbf{a}), \tag{2}$$

where $\mathbf{W}_a$, $\mathbf{W}_k$ and $\mathbf{W}_q$ are weight matrices, and a_i represents the i-th element in $\mathbf{a}$. Finally, the attention module produces the attended feature $\hat{\mathbf{v}}$ by accumulating all values $\mathbf{V} = \{\mathbf{v}_i\}_{i=1}^n$ with contextual attention weights: $\hat{\mathbf{v}} = \sum_{i=1}^{n} \alpha_i \mathbf{v}_i$. It can be denoted as:

$$\mathbf{V} = \mathrm{Att}(\mathbf{Q}, \mathbf{K}, \mathbf{V}). \tag{3}$$

$\mathbf{H_I}$ and $\mathbf{H_S}$ are fed into the CAL to strengthen both the intent and slot features in a mutual way. Same as Vaswani et al. (2017), we first map the matrix $\mathbf{H_I}$ and $\mathbf{H_S}$ to queries($\mathbf{Q_I^{(1)}}, \mathbf{Q_S^{(1)}}$), keys($\mathbf{K_I^{(1)}}, \mathbf{K_S^{(1)}}$) and values($\mathbf{V_I^{(1)}}, \mathbf{V_S^{(1)}}$) matrices by using different linear projections. Then we take $\mathbf{Q_I^{(1)}} \in \mathbb{R}^{n \times d}$, $\mathbf{K_S^{(1)}} \in \mathbb{R}^{n \times d}$ and $\mathbf{V_S^{(1)}} \in \mathbb{R}^{n \times d}$ as queries, keys and values, respectively, acquiring the enhanced values:

$$\begin{aligned} \hat{\mathbf{V}_\mathbf{I}^{(1)}} &= \mathrm{Att}(\mathbf{Q_I^{(1)}}, \mathbf{K_S^{(1)}}, \mathbf{V_S^{(1)}}), \\ \mathbf{H_I^{(1)}} &= \mathrm{LN}(\mathbf{H_I} + \hat{\mathbf{V}_\mathbf{I}^{(1)}}), \end{aligned} \tag{4}$$

where LN represents the layer normalization. Similarly, we take $\mathbf{Q_S}$ as queries, $\mathbf{K_I}$ as keys and $\mathbf{V_I}$ as values to obtain $\mathbf{H_S^{(1)}}$. We can obtain the enhanced intent features $\mathbf{H_I^{(N)}} \in \mathbb{R}^{n \times d}$ and slot features $\mathbf{H_S^{(N)}} \in \mathbb{R}^{n \times d}$ after repeating the above process N times.

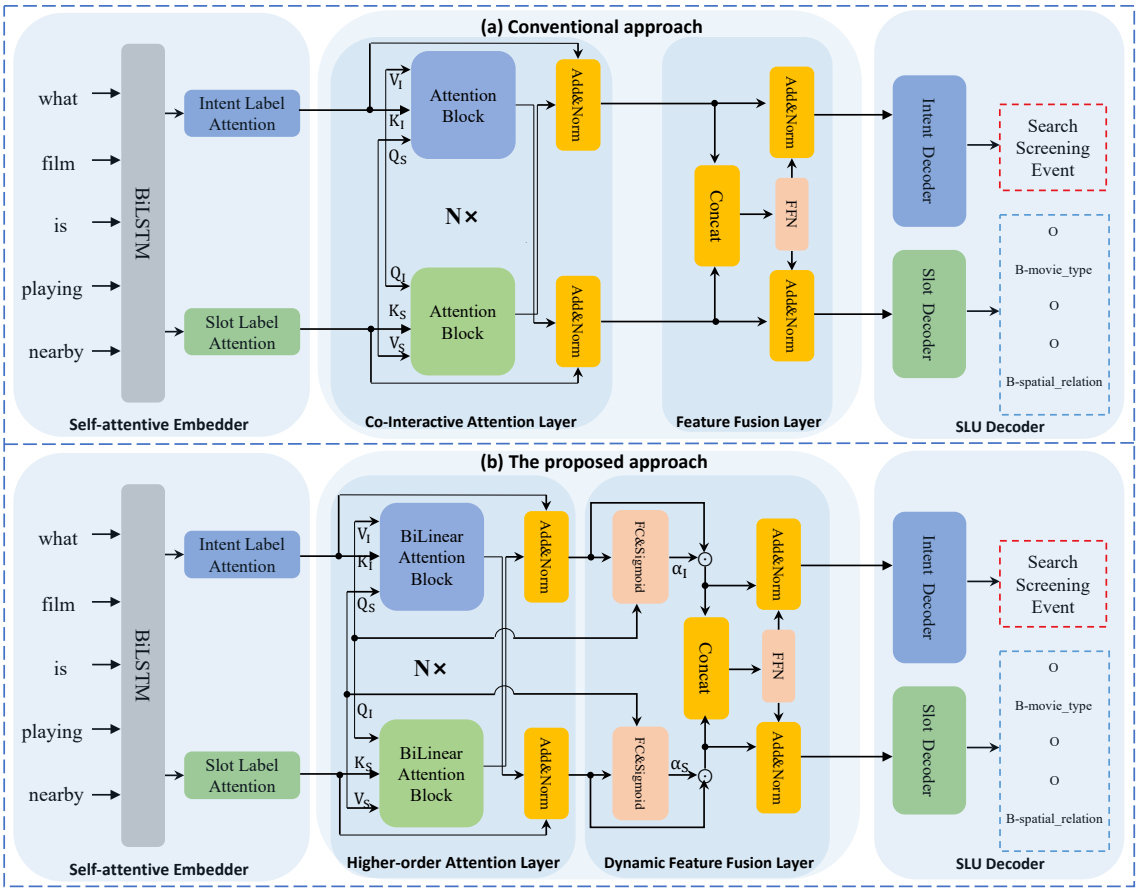

Figure 1: (a) Conventional approach consists of four parts, i.e., Self-attentive Embedder, Co-Interactive Attention Laye (CAL), Feature Fusion Laye (FFL) and SLU Decoder. (b) By replacing the CAL and FFL with HAL and DFFL, respectively, we obtain the proposed HAN. HAN can model higher-order feature interactions via stacking multiple layers of HAL or equipping it with Exponential Linear Unit (ELU) in a parameter-free fashion.

Feature Fusion Layer (FFL) In this part, we extend Feed-Forward Network layer to implicitly fuse intent and slot information, we first concatenate $\mathbf{H_I^{(N)}}$ and $\mathbf{H_S^{(N)}}$ to combine the intent and slot information:

$$\mathbf{H_{IS}} = [\mathbf{H_I^{(N)}}, \mathbf{H_S^{(N)}}], \tag{5}$$

where $[\cdot, \cdot]$ indicates concatenation. Then, we adopt the Feed-Forward Network (FFN) to acquire the updated intent features $\hat{\mathbf{H}}_\mathbf{I}^{(\mathbf{N})} \in \mathbb{R}^{n \times d}$ and slot features $\hat{\mathbf{H}}_\mathbf{S}^{(\mathbf{N})} \in \mathbb{R}^{n \times d}$:

$$\begin{aligned} \hat{\mathbf{H}}_\mathbf{I}^{(\mathbf{N})} &= \mathrm{LN}(\mathrm{FFN}(\mathbf{H_{IS}}) + \mathbf{H_I^{(N)}}), \\ \hat{\mathbf{H}}_\mathbf{S}^{(\mathbf{N})} &= \mathrm{LN}(\mathrm{FFN}(\mathbf{H_{IS}}) + \mathbf{H_S^{(N)}}). \end{aligned} \tag{6}$$

SLU Decoder For the intent detection, we follow Kim (2014) to employ the maxpooling on $\hat{\mathbf{H}}_\mathbf{I}^{(\mathbf{N})}$ to obtain $\boldsymbol{c}$, which is used to predict the intent label: $\mathbf{o^I} \sim \hat{\mathbf{y}}^\mathbf{I} = \mathrm{softmax}\left(\mathbf{W^I}\boldsymbol{c} + \mathbf{b_I}\right)$.

For the slot filling, we apply a standard CRF layer (Niu et al. 2019) to model the dependency between labels, and then predict the label sequence:

$$P(\hat{\mathbf{y}}|\mathbf{O_S}) = \frac{\sum_{i=1} \exp f(y_{i-1}, y_i, \mathbf{O_S})}{\sum_{y'} \sum_{i=1} \exp f(y'_{i-1}, y'_i, \mathbf{O_S})}, \tag{7}$$

where y' represents an arbitary label sequence, $\mathbf{O_S} = \mathbf{W^S}\hat{\mathbf{H}}_\mathbf{S}^{(\mathbf{N})} + \mathbf{b_S}$ and $f(y'_{i-1}, y'_i, \mathbf{O_S})$ computes the transition score from y_{i-1} to y_i.

The Proposed Approach

The proposed approach is shown in Figure 1(b), we replace CAL and FFL with HAL and DFFL, respectively, and thus obtain the proposed Higher-order Attention Network, i.e., HAN. The HAL is proposed to build higher-order feature interactions, and the DFFL can fuse intent and slot features in a more reasonable way. Before introducing HAL and DFFL, we first describe the proposed BiLinear attention block illustrated in Figure 2.

BiLinear attention block As can be seen above, the conventional attention can only exploit the first-order feature

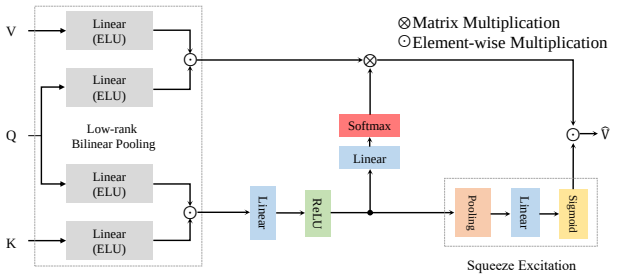

Figure 2: The proposed BiLinear attention block, which is based on the low-rank bilinear pooling (Kim et al. 2016).

interactions, which may restrict the capacity of features representation in the SLU models. Inspired by the successful application of bilinear pooling in the field of Computer Vision research (Fukui et al. 2016; Gao et al. 2016; Kim, Jun, and Zhang 2018), we propose the BiLinear attention block. Such a design of the BiLinear attention block strengthens the representative capacity of the output attended feature by exploiting higher-order interactions between the input intent and slot features.

Consider that there is a query $\mathbf{q} \in \mathbb{R}^d$, a set of keys $\mathbf{K} = \{\mathbf{k}_i\}_{i=1}^n$, and a set of values $\mathbf{V} = \{\mathbf{v}_i\}_{i=1}^n$, where $\mathbf{k}_i, \mathbf{v}_i \in \mathbb{R}^d$ denote the i-th key/value pair. A joint bilinear query-key representation $\mathbf{B}_{ki} \in \mathbb{R}^d$ to model the second-order feature interactions between query and keys are achieved by the low-rank bilinear pooling operation:

$$\mathbf{B}_{ki} = \mathrm{ReLU}(\mathbf{W}_{qk}\mathbf{q}) \odot \mathrm{ReLU}(\mathbf{W}_k\mathbf{k}_i), \tag{8}$$

where $\mathbf{W}_{qk}, \mathbf{W}_k \in \mathbb{R}^{d\times d}$ are two weight matrices.

Next, two types of bilinear attention distributions are obtained to aggregate both contextual and channel-wise information within all values by using all bilinear query-key representations $\{\mathbf{B}_{ki}\}_{i=1}^n$. Technically, the contextual bilinear attention distribution is introduced by projecting each bilinear query-key representation into the corresponding attention weight via two fully-connected layers, followed by a softmax layer for normalization:

$$\begin{aligned} \mathbf{B}'_{ki} &= \mathrm{ReLU}(\mathbf{W}_{Bk}\mathbf{B}_{ki}), \\ b_{si} &= \mathbf{W}_b\mathbf{B}'_{ki}, \beta_{\mathbf{s}} = \mathrm{softmax}(\mathbf{b}_{\mathbf{s}}), \end{aligned} \tag{9}$$

where $\mathbf{W}_{Bk} \in \mathbb{R}^{d\times d}$ and $\mathbf{W}_b \in \mathbb{R}^{1\times d}$ are weight matrices, $\mathbf{B}'_{ki}$ is the transformed bilinear query-key representation, and b_{si} is the i-th element in $\mathbf{b}_{\mathbf{s}}$. Here each element β_{si} in $\beta_{\mathbf{s}}$ denotes the normalized contextual attention weight for each key/value pair. Meanwhile, we perform a squeeze-excitation operation over over all transformed bilinear query-key representations $\{\mathbf{B}'_{ki}\}_{i=1}^n$ for channel-wise attention measurement. Concretely, the operation of squeeze aggregates all transformed bilinear query-key representations via average pooling, leading to a channel descriptor:

$$\overline{\mathbf{B}} = \frac{1}{n}\sum_{i=1}^{n}\mathbf{B}'_{ki}. \tag{10}$$

After that, the followed excitation operation produces channel-wise attention distribution $\beta_{\mathbf{c}}$ by leveraging the self-gating mechanism with a sigmoid over the $\overline{\mathbf{B}}$:

$$\mathbf{b}_{\mathbf{c}} = \mathbf{W}_c\overline{\mathbf{B}}, \beta_{\mathbf{c}} = \sigma(\mathbf{b}_{\mathbf{c}}), \tag{11}$$

where σ is the sigmoid activation and $\mathbf{W}_c \in \mathbb{R}^{d\times d}$ is a weight matrix.

Finally, our BiLinear attention block generates the attended value feature $\hat{\mathbf{v}}_i$ by accumulating the enhanced bilinear values with contextual and channel-wise bilinear attention:

$$\begin{aligned} \hat{\mathbf{v}}_i &= \beta_{\mathbf{c}} \odot \sum_{i=1}^{n}\beta_{si}\mathbf{B}_{vi}, \\ \mathbf{B}_{vi} &= \mathrm{ReLU}(\mathbf{W}_{qv}\mathbf{q}) \odot \mathrm{ReLU}(\mathbf{W}_v\mathbf{v}_i), \end{aligned} \tag{12}$$

where $\mathbf{B}_{vi}$ denotes the enhanced value of bilinear pooling on query $\mathbf{q}$ and each value $\mathbf{v}_i$, $\mathbf{W}_{qv} \in \mathbb{R}^{d\times d}$ and $\mathbf{W}_v \in \mathbb{R}^{d\times d}$ are weight matrices. As such, BiLinear attention block produces more representative attended features since higher-order feature interactions are exploited via bilinear pooling. We iterate the above process n times with $\mathbf{Q} = \{\mathbf{q}_i\}_{i=1}^n$, and get a set of values $\hat{\mathbf{V}} = \{\hat{\mathbf{v}}_i\}_{i=1}^n$, we denote it as:

$$\hat{\mathbf{V}} = \mathrm{Att}_{bilinear}(\mathbf{Q}, \mathbf{K}, \mathbf{V}), \tag{13}$$

where $\hat{\mathbf{V}} \in \mathbb{R}^{n\times d}$ is the enhanced features with second-order attention feature interactions. To get higher-order feature interactions, we further iterate the above process of bilinear attention measurement and feature aggregation using a stack of our BiLinear attention blocks, i.e., we can get $2N^{th}$-order feature interactions by repeating the process N times:

$$\hat{\mathbf{V}^{(\mathbf{N})}} = \mathrm{Att}_{bilinear}(\mathbf{Q}^{(\mathbf{N})}, \mathbf{K}^{(\mathbf{N})}, \mathbf{V}^{(\mathbf{N})}). \tag{14}$$

Although it is possible to model any high-order feature interactions by stacking enough BiLinear attention blocks theoretically, considering that there will be over-fitting in practice, there will be an optimal number of stacked layers and an optimal order. We will delve deeper into them in the *Discussion* part.

Fortunately, by equipping the block with Exponential Linear Unit (ELU) (Barron 2017), it can model infinity-order feature interactions, which can be proved via Taylor expansion of each element in the bilinear vector after exponential transformation.

For instance, given two vectors A and B, their exponential bilinear pooling can be estimated using the Taylor expansion:

$$\begin{aligned} &\exp\left(\mathrm{W}_A\mathrm{A}\right) \odot \exp\left(\mathrm{W}_B\mathrm{B}\right) \\ &= \left[\exp\left(\mathrm{W}_A^1\mathrm{A}\right) \odot \exp\left(\mathrm{W}_B^1\mathrm{B}\right), \ldots, \exp\left(\mathrm{W}_A^D\mathrm{A}\right) \odot \exp\left(\mathrm{W}_B^D\mathrm{B}\right)\right] \\ &= \left[\exp\left(\mathrm{W}_A^1\mathrm{A} + \mathrm{W}_B^1\mathrm{B}\right), \ldots, \exp\left(\mathrm{W}_A^D\mathrm{A} + \mathrm{W}_B^D\mathrm{B}\right)\right] \\ &= \left[\sum_{p=0}^{\infty} r_p^1\left(\mathrm{W}_A^1\mathrm{A} + \mathrm{W}_B^1\mathrm{Y}\right)^p, \ldots, \sum_{p=0}^{\infty} r_p^D\left(\mathrm{W}_A^D\mathrm{A} + \mathrm{W}_B^D\mathrm{B}\right)^p\right], \end{aligned}$$

where W_A and W_B are weight matrices, D denotes the dimension of bilinear vector, W_A^i/W_B^i is the i-th row in W_A/W_B.

Higher-order Attention Layer (HAL) Followed by equation (1), $\mathbf{H_I}$ and $\mathbf{H_S}$ are further fed into the our Higher-order Attention Layer to strengthen both the intent and slot features via capturing higher-order feature interactions between them. Formally, the HAL is composed of a stack of N identical sublayers ($N = 2$). Each sublayer consists of Bi-Linear attention block (ELU) and layer normalization. Since that we just replace the CAL with HAL, so the equation (4) should be replaced with the following formulas:

$$\begin{aligned}\hat{\mathbf{V}_\mathbf{I}^{(1)}} &= \mathrm{Att}_{bilinear}(\mathbf{Q_I^{(1)}}, \mathbf{K_S^{(1)}}, \mathbf{V_S^{(1)}}), \\ \mathbf{H_I^{(1)}} &= \mathrm{LN}(\mathbf{H_I} + \hat{\mathbf{V}_\mathbf{I}^{(1)}}),\end{aligned} \tag{15}$$

similarly, we take $\mathbf{Q_S^{(1)}}$ as queries, $\mathbf{K_I^{(1)}}$ as keys and $\mathbf{V_I^{(1)}}$ as values to obtain $\mathbf{H_S^{(1)}}$.

After repeating N times, we can obtain the enhanced intent features $\mathbf{H_I^{(N)}} \in \mathbb{R}^{n \times d}$ and slot features $\mathbf{H_S^{(N)}} \in \mathbb{R}^{n \times d}$, which are endowed with the higher-order feature interactions in between.

Dynamic Feature Fusion Layer (DFFL) Inspired by Cornia et al. (2020), we proposed a more reasonable way to fuse intent and slot features. First, we compute two weight matrices $\alpha_\mathbf{I}$ and $\alpha_\mathbf{S}$ which reflect the relevance between the output and the input query of the last sublayer in the HAL, and then obtain the fused features $\mathbf{H_{IS}}$, which can be defined as follows:

$$\begin{aligned}\alpha_\mathbf{I} &= \sigma(\mathbf{W}_I[\mathbf{Q_I^{(N)}}, \mathbf{H_I^{(N)}}] + b_I), \\ \alpha_\mathbf{S} &= \sigma(\mathbf{W}_S[\mathbf{Q_S^{(N)}}, \mathbf{H_S^{(N)}}] + b_S), \\ \mathbf{H_{IS}} &= [\alpha_\mathbf{I} \odot \mathbf{H_I^{(N)}}, \alpha_\mathbf{S} \odot \mathbf{H_S^{(N)}}],\end{aligned} \tag{16}$$

where $\odot$ denotes element-wise multiplication; $\mathbf{W}_I$ and $\mathbf{W}_S$ are both $2d \times d$ embedding matrices, b_I and b_S are biases. Then, same as equation (6), we acquire the updated intent features $\hat{\mathbf{H}_\mathbf{I}}^{(\mathbf{N})} \in \mathbb{R}^{n \times d}$ and slot features $\hat{\mathbf{H}_\mathbf{S}}^{(\mathbf{N})} \in \mathbb{R}^{n \times d}$.

Joint Training Strategy

We adopt a joint learning scheme to optimize intent detection and slot filling simultaneously as Goo et al. (2018). Specifically, a cross-entropy loss is used for intent detection: $\mathcal{L}_1 = -\sum_{j=1}^{m} \hat{\mathbf{y}}^{\mathbf{I},j} \log(\mathbf{y}^{\mathbf{I},j})$. Similarly, the slot filling objective is: $\mathcal{L}_2 = -\sum_{j=1}^{m} \sum_{i=1}^{n_S} \hat{\mathbf{y}}_i^{\mathbf{S},j} \log(\mathbf{y}_i^{\mathbf{S},j})$, where $\hat{\mathbf{y}}_i^{\mathbf{I},j}$ and $\hat{\mathbf{y}}_i^{\mathbf{S},j}$ are the gold intent label and gold slot label separately; n_S is the number of slot labels and m is the number of training data.

The final joint objective is formulated as: $\mathcal{L}_{total} = \mathcal{L}_1 + \mathcal{L}_2$. Through the joint loss function, the parameters in our model will be optimized based on considering the effect of the mutual interaction between two subtasks.

Experiments

Datasets

We conduct experiments on two benchmark datasets, i.e., SNIPS and ATIS. SNIPS has 13084 utterances for training, 700 for validation, and 700 for testing. ATIS has 4478 utterances for training, 500 utterances for validation, and 893 utterances for testing. Both datasets are used in our paper following the same format and partition as in Goo et al. (2018).

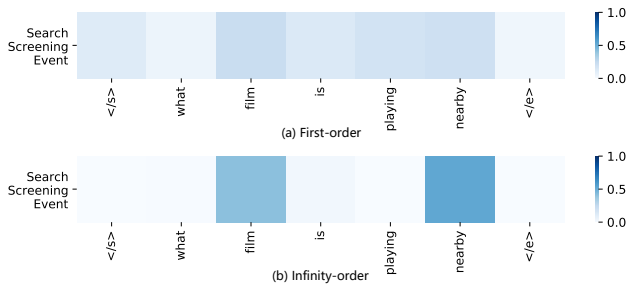

Figure 3: Visualization of the first-order attention (a) and the infinity-order attention (b). The utterance is acquired from the SNIPS dataset.

Experimental Settings

Following previous work, we adopt the RAdam (Liu et al. 2020) optimizer to update the parameters, with a mini-batch size of 32 and initial learning rate of 0.001. We use 300d GloVe pre-trained vector (Pennington, Socher, and Manning 2014) as the initialization embedding. The hidden dimensionality d is set as 128. Three evaluation metrics are used for the SLU task. The performance of intent detection is measured by accuracy, while slot filling is evaluated with the F1 score, and the sentence-level semantic frame parsing using overall accuracy which represents both intent and slot are correctly recognized for an utterance. We select the model which works the best on the dev set, and then evaluate it on the test set. The model was implemented in PyTorch and trained on a single NVIDIA GeForce GTX 2080Ti GPU.

Experimental Results

Table 2 shows the main experiment results, we can see that our HAN significantly outperforms all the baselines and achieves competitive performance.

For the SNIPS dataset, compared with the best prior work *Co-Interactive*, we achieved 0.83% improvement on Slot (F1) score, 0.41% improvement on Intent (Acc) and 2.68% improvement on Overall (Acc). For the ATIS dataset, we achieve 0.65% improvement on Slot (F1) score, 0.39% improvement on Intent (Acc) and 1.78% improvement on Overall (Acc). This again confirms the advantage of capturing the higher-order feature interactions among intent and slot via our BiLinear attention block.

Besides, we also conduct experiments to use the strong pre-trained model BERT (Devlin et al. 2019) to boost SLU performance. Technically, we just replace the Self-attentive Embedder by $\mathrm{BERT}_{\mathrm{BASE}}$ model with the fine-tuning approach and keep other components as same with our framework. We can see that HAN has been further improved on both two datasets. It demonstrates that our framework is effective with BERT.

Model	SNIPS			ATIS		
	Slot (*F1*)	Intent (*Acc*)	Overall (*Acc*)	Slot (*F1*)	Intent (*Acc*)	Overall (*Acc*)
Slot-Gated Full Atten (Goo et al. 2018)	88.80	97.00	75.50	94.80	93.60	82.20
Self-Attentive Model (Li, Li, and Qi 2018)	90.00	97.50	81.00	95.10	96.80	82.20
Bi-Model (Wang, Shen, and Jin 2018)	93.50	97.20	83.80	95.50	96.40	85.70
CAPSULE-NLU (Zhang et al. 2019)	91.80	97.30	80.90	95.20	95.00	83.40
SF-ID Network (E et al. 2019)	90.50	97.00	78.40	95.60	96.60	86.00
Stack-Propagation (Qin et al. 2019)	94.20	98.00	86.90	95.90	96.90	86.50
Graph-LSTM (Zhang et al. 2020)	95.30	98.29	89.71	95.91	97.20	87.57
Co-Interactive (Qin et al. 2021)	95.35	98.71	89.12	95.47	97.65	86.69
Baseline (BiLSTM + Decoder)	94.19	97.79	85.86	95.32	95.63	84.99
+ (Label attention + shallow concat)	94.39	98.03	87.89	95.55	97.52	85.89
+ Conventional attention (first-order)	95.37	98.34	88.12	95.64	97.43	87.01
+ BiLinear attention block (second-order)	95.35	98.43	88.57	95.83	97.43	87.32
+ Dynamic Feature Fusion (second-order)	95.57	98.57	89.43	95.88	97.56	87.57
+ ELU (Infinity-order)	96.01	98.69	90.43	95.95	97.89	88.12
HAN (Ours)	**96.18**	**99.12**	**91.80**	**96.12**	**98.04**	**88.47**
HAN + $\text{BERT}_{\text{BASE}}$	97.66	99.23	93.54	96.83	98.54	89.31

Table 2: Slot filling and intent detection results on two datasets. Our HAN achieves competitive performance on both two benchmark datasets. Then we incorporate the pre-trained model ($\text{BERT}_{\text{BASE}}$) in HAN, which can further improve the performance. The ablation experiments are designed to explore the effect of every component in HAN, and the sublayer number of HAL is kept as one. The *"shallow concat"* means directly concatenate two features without dynamic feature fusion.

Model	HAL	SNIPS			ATIS		
		Slot(*F1*)	Intent(*Acc*)	Overall(*Acc*)	Slot(*F1*)	Intent(*Acc*)	Overall(*Acc*)
Stack-Propagation (Qin et al. 2019)	×	94.20	98.00	86.90	95.90	96.90	86.50
	✓	**94.70**	**98.20**	**87.20**	**96.20**	**97.50**	**87.40**
Co-Interactive (Qin et al. 2021)	×	95.35	**98.71**	89.12	95.47	97.65	86.69
	✓	**95.49**	98.57	**89.86**	**95.98**	**97.87**	**87.35**
HAN (Ours)	×	95.43	98.57	89.29	95.87	97.42	87.12
	✓	**96.18**	**99.12**	**91.80**	**96.12**	**98.04**	**88.47**

Table 3: Impact of higher-order attention on different baselines, i.e., Stack Propagation, Co-Interactive, and our HAN. The best results compared for every baseline on both datasets are in bold.

For the ablation studies, we can see that as adding each key component of HAN gradually, the performance becomes better, and it gets improvement most when equipping with ELU (4.57% and 3.13% improvement compared to baseline in overall accuracy on the SNIPS and ATIS dataset, respectively). The performance improves gradually demonstrates the positive effect of each key component, and the most improvement brought by ELU proves the core advantage of exploiting higher and even infinity-order feature interactions between intent and slot.

Discussion

Visualization of Attention

To clearly show what the higher-order attention has learned, we visualize the first-order attention distribution in Eq. (2) and the infinity-order attention distribution in Eq. (8) for comparison. In particular, we visualize the attention distribution of the intent feature to each token of slot features. As can be seen in Figure 3, where we use the utterance *"What film is playing nearby"* from the SNIPS dataset. The proposed higher-order attention focus more on the keyword *"film"* and *"nearby"*, showing a better attention capture ability compared to the conventional first-order attention.

Robustness towards Learning Rate

To verify the robustness of higher-order attention towards hyper-parameter, e.g., learning rate, we conduct the following experiments. From Figure 4, using the overall Accuracy as metric, we show that under same experimental settings, infinity-order model performs better than the first-order model under different learning rate. Besides, we find that under reasonable and task-specific range of the learning rate, i.e., 1e-4 to 1e-2, the higher-order based model

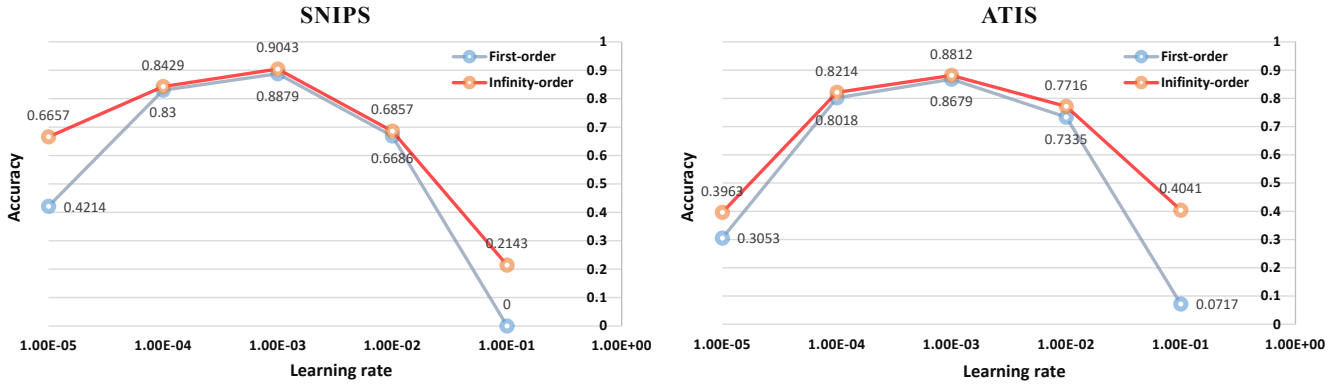

Figure 4: Performance of the infinity-order model (HAN) and first-order model under different learning rate. The first-order model is acquired by replacing our higher-order attention with conventional attention.

L	ELU	SNIPS			ATIS		
		Slot	Intent	Overall	Slot	Intent	Overall
1	×	95.57	98.57	89.43	95.88	97.56	87.57
	✓	96.01	98.69	90.43	95.95	97.89	88.12
2	×	**95.86**	**98.57**	**89.71**	**95.92**	**97.76**	**87.79**
	✓	**96.18**	**99.12**	**91.80**	**96.12**	**98.04**	**88.47**
3	×	95.65	98.29	89.57	95.75	97.54	87.12
	✓	95.70	98.57	89.86	95.75	97.42	87.23
4	×	95.51	98.00	89.00	95.75	97.31	87.01
	✓	95.65	98.29	89.11	95.77	97.42	87.01
5	×	95.12	97.86	88.86	95.58	97.54	86.67
	✓	95.32	98.14	88.86	95.83	97.31	86.90

Table 4: Effect of the sublayer number (L) of HAL on the HAN performance. We can see that when the number of HAL is 2, the HAN achieves the best performance, whether equipped the model with ELU or not.

performs slightly and consistently better than the first-order based model. When the learning rate is out of this range, i.e., bigger than 1e-2 or smaller than 1e-4, the performance of the first-order based model occurs to crack down quickly and it even drops to 0 when the learning rate is 0.1. Oppositely, the higher-order based model, though also drops down when the learning reaches is set out of reasonable range, can still keep considerable performance compared to the first-order base model, and thus shows its robustness to the extreme case towards the optimized learning rate.

Generalization Analysis

To explore the generalization of the proposed higher-order attention, we further incorporate Higher-order Attention Layer into two existing baselines (i.e., Stack-Propagation and Co-Interactive). For Stack-Propagation, Higher-order Attention Layer is inserted after it's Self-Attentive Encoder. For Co-Interactive, we just replace it's Co-Interactive Attention Layer with the Higher-order Attention Layer. Table 3 shows that baselines with infinity-order attention, i.e., HAL, perform better than that with first-order attention in most cases. This further verifies the generalization of the effectiveness of the higher-order attention on the SLU task.

Discussion on the sublayer number of HAL

Considering that there will be over-fitting when there are too many BiLinear attention blocks stacked. Thus, to find the best sublayer number of HAL, we designed experiments on both two datasets by varying the HAL's sublayer number from one to five while keeping others consistent.

From Table 4, we can see that when the number of sublayers in HAL is two, performance of HAN on both datasets get the best, whether equipped the model with ELU. So we set the sublayer number of HAL as two mentioned in *Approach* part ($N = 2$). When the number of sublayers is more than two, the performance drops gradually as it increases. Therefore, we have enough reasons to infer that the increased parameters by stacking more blocks might result in over-fitting, which somewhat hinders the exploitation of higher-order interaction in this way.

Conclusion

In this paper, we propose to build the second-order interactions between intent and slot features for SLU task by introducing a novel BiLinear attention block, and thus more discriminative intent and slot representations can be utilized when model the the intent detection and slot filling tasks. Besides, higher and even infinity-order feature interactions are further proposed via stacking multiple BiLinear attention blocks and equipping the block with ELU activation. Furthermore, we introduce the HAN, which achieves a new state-of-the-art result on both two benchmark SLU datasets. We also validate the components of our model through ablation studies. The detailed discussion proves the effectiveness of the higher-order attention in terms of robustness and generalization. We believe that the proposed high-order attention can be applied to other similar Natural Language Processing tasks.

References

Barron, J. T. 2017. Continuously Differentiable Exponential Linear Units. *CoRR*, abs/1704.07483.

Chen, B.; Deng, W.; and Hu, J. 2019. Mixed high-order attention network for person re-identification. In *ICCV*.

Cornia, M.; Stefanini, M.; Baraldi, L.; and Cucchiara, R. 2020. Meshed-memory transformer for image captioning. In *CVPR*.

Coucke, A.; Saade, A.; Ball, A.; Bluche, T.; Caulier, A.; Leroy, D.; Doumouro, C.; Gisselbrecht, T.; Caltagirone, F.; Lavril, T.; Primet, M.; and Dureau, J. 2018. Snips Voice Platform: an embedded Spoken Language Understanding system for private-by-design voice interfaces. *CoRR*, abs/1805.10190.

Cui, L.; and Zhang, Y. 2019. Hierarchically-refined label attention network for sequence labeling. *arXiv preprint arXiv:1908.08676*.

Devlin, J.; Chang, M.; Lee, K.; and Toutanova, K. 2019. BERT: Pre-training of Deep Bidirectional Transformers for Language Understanding. In *NAACL-HLT*.

E, H.; Niu, P.; Chen, Z.; and Song, M. 2019. A Novel Bi-directional Interrelated Model for Joint Intent Detection and Slot Filling. In *ACL*.

Fukui, A.; Park, D. H.; Yang, D.; Rohrbach, A.; Darrell, T.; and Rohrbach, M. 2016. Multimodal Compact Bilinear Pooling for Visual Question Answering and Visual Grounding. In *EMNLP*.

Gao, Y.; Beijbom, O.; Zhang, N.; and Darrell, T. 2016. Compact bilinear pooling. In *CVPR*.

Goo, C.-W.; Gao, G.; Hsu, Y.-K.; Huo, C.-L.; Chen, T.-C.; Hsu, K.-W.; and Chen, Y.-N. 2018. Slot-gated modeling for joint slot filling and intent prediction. In *ACL*.

Hemphill, C. T.; Godfrey, J. J.; and Doddington, G. R. 1990. The ATIS Spoken Language Systems Pilot Corpus. In *HLT*.

Hou, L.; Huang, Z.; Shang, L.; Jiang, X.; Chen, X.; and Liu, Q. 2020. DynaBERT: Dynamic BERT with Adaptive Width and Depth. In *NeurIPS*.

Huang, Z.; Hou, L.; Shang, L.; Jiang, X.; Chen, X.; and Liu, Q. 2021a. GhostBERT: Generate More Features with Cheap Operations for BERT. In *ACL/IJCNLP*.

Huang, Z.; Liu, F.; Wu, X.; Ge, S.; Wang, H.; Fan, W.; and Zou, Y. 2021b. Audio-Oriented Multimodal Machine Comprehension via Dynamic Inter- and Intra-modality Attention. In *AAAI*.

Huang, Z.; Liu, F.; Zhou, P.; and Zou, Y. 2021c. Sentiment Injected Iteratively Co-Interactive Network for Spoken Language Understanding. In *ICASSP*.

Huang, Z.; Liu, F.; and Zou, Y. 2020. Federated Learning for Spoken Language Understanding. In *COLING*.

Kim, J.-H.; Jun, J.; and Zhang, B.-T. 2018. Bilinear attention networks. *arXiv preprint arXiv:1805.07932*.

Kim, J.-H.; On, K.-W.; Lim, W.; Kim, J.; Ha, J.-W.; and Zhang, B.-T. 2016. Hadamard product for low-rank bilinear pooling. *arXiv preprint arXiv:1610.04325*.

Kim, Y. 2014. Convolutional Neural Networks for Sentence Classification. In *EMNLP*.

Li, C.; Li, L.; and Qi, J. 2018. A Self-Attentive Model with Gate Mechanism for Spoken Language Understanding. In *EMNLP*.

Lin, T.; RoyChowdhury, A.; and Maji, S. 2015. Bilinear CNN Models for Fine-Grained Visual Recognition. In *ICCV*.

Liu, B.; and Lane, I. 2016. Joint Online Spoken Language Understanding and Language Modeling With Recurrent Neural Networks. In *SIGDIAL*.

Liu, L.; Jiang, H.; He, P.; Chen, W.; Liu, X.; Gao, J.; and Han, J. 2020. On the Variance of the Adaptive Learning Rate and Beyond. In *ICLR*.

Niu, P.; Chen, Z.; Song, M.; et al. 2019. A novel bi-directional interrelated model for joint intent detection and slot filling. *arXiv preprint arXiv:1907.00390*.

Pennington, J.; Socher, R.; and Manning, C. D. 2014. Glove: Global vectors for word representation. In *EMNLP*.

Qin, L.; Che, W.; Li, Y.; Wen, H.; and Liu, T. 2019. A Stack-Propagation Framework with Token-Level Intent Detection for Spoken Language Understanding. In *EMNLP/IJCNLP*.

Qin, L.; Liu, T.; Che, W.; Kang, B.; Zhao, S.; and Liu, T. 2021. A co-interactive transformer for joint slot filling and intent detection. In *ICASSP*.

Ramshaw, L. A.; and Marcus, M. 1995. Text Chunking using Transformation-Based Learning. In *VLC@ACL*.

Vaswani, A.; Shazeer, N.; Parmar, N.; Uszkoreit, J.; Jones, L.; Gomez, A. N.; Kaiser, L.; and Polosukhin, I. 2017. Attention is All you Need. In *NIPS*.

Wang, Y.; Shen, Y.; and Jin, H. 2018. A Bi-Model Based RNN Semantic Frame Parsing Model for Intent Detection and Slot Filling. In *NAACL-HLT*.

Xia, C.; Zhang, C.; Yan, X.; Chang, Y.; and Yu, P. S. 2018. Zero-shot User Intent Detection via Capsule Neural Networks. In *EMNLP*.

Zhang, C.; Du, N.; Fan, W.; Li, Y.; Lu, C.; and Yu, P. S. 2017. Bringing semantic structures to user intent detection in online medical queries. In *BigData*.

Zhang, C.; Fan, W.; Du, N.; and Yu, P. S. 2016. Mining User Intentions from Medical Queries: A Neural Network Based Heterogeneous Jointly Modeling Approach. In *WWW*.

Zhang, C.; Li, Y.; Du, N.; Fan, W.; and Yu, P. S. 2019. Joint Slot Filling and Intent Detection via Capsule Neural Networks. In *ACL*.

Zhang, L.; Ma, D.; Zhang, X.; Yan, X.; and Wang, H. 2020. Graph LSTM with Context-Gated Mechanism for Spoken Language Understanding. In *AAAI*.

Zhang, X.; and Wang, H. 2016. A joint model of intent determination and slot filling for spoken language understanding. In *IJCAI*.

Zhou, P.; Huang, Z.; Liu, F.; and Zou, Y. 2020. PIN: A Novel Parallel Interactive Network for Spoken Language Understanding. In *ICPR*.